

Figure S1, Ichikawa et.al.

**Supplementary figure S1. Characterization of SORBS-reexpressing cells.** (A) DKO MEFs were isolated from DKO mice and subjected to lentivirus infection to establish TKO MEFs. Expression of SORBS proteins was examined by immunoblotting using the indicated antibodies. Vinculin was used as a loading control. The lysate of astrocytes served as a reference sample, which expressed all SORBS proteins. (B) The knockdown efficiency of shRNA against ArgBP2 was confirmed by immunoblotting using mouse mesenchymal cell lines ATDC5 that were differentiated to chondrocyte. ATDC5 cells were infected with lentivirus expressing control shRNA or shRNA against ArgBP2. Two different levels of multiplicity of infection (MOI) were tested, and ArgBP2 was knocked down in a MOI-dependent manner. (C-E) Related to Fig. 2, specificity of anti-SORBS proteins was confirmed. Each anti-SORBS antibodies did not cross-react to other SORBS proteins under this condition. Note that anti-ArgBP2 antibody stained the punctate structures within the nucleus nonspecifically. (F) SORBS-reexpressing cells cultured on collagen coated dishes were lysed and subjected to SDS-PAGE. Expression of vinculin and paxillin were examined by immunoblotting using the indicated antibodies.  $\beta$ -actin was used as a loading control.

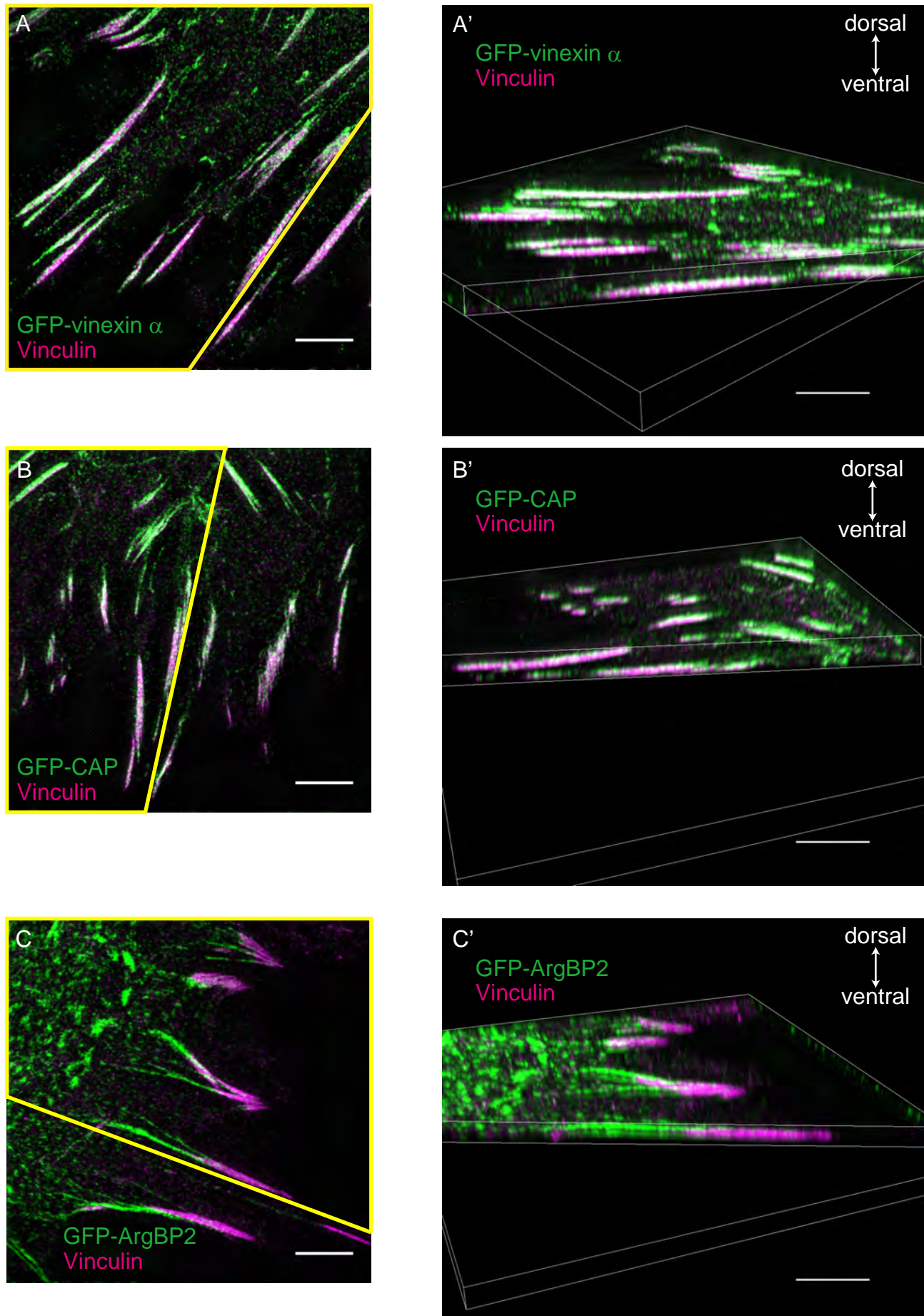


Figure S2, Ichikawa et.al.

**Supplementary figure S2. Super-resolution microscopy provides the fine localization of SORBS proteins.** TKO MEFs reexpressing GFP-tagged SORBS proteins were cultured on coverslips were fixed, followed by immunostaining using anti-vinculin antibody. Fifteen slice images were acquired with Z-steps of 0.12  $\mu\text{m}$  for each XY position by using 3D-SIM super-resolution microscopy. (A-C) Images are displayed as the maximum intensity projection of Z-stack images. Scale bars, 5  $\mu\text{m}$ . The yellow line shows an orthogonal cut edge for 3D volume visualization. (A'-C') Images are displayed as 3D volume reconstructions. Scale bars, 5 $\mu\text{m}$ .

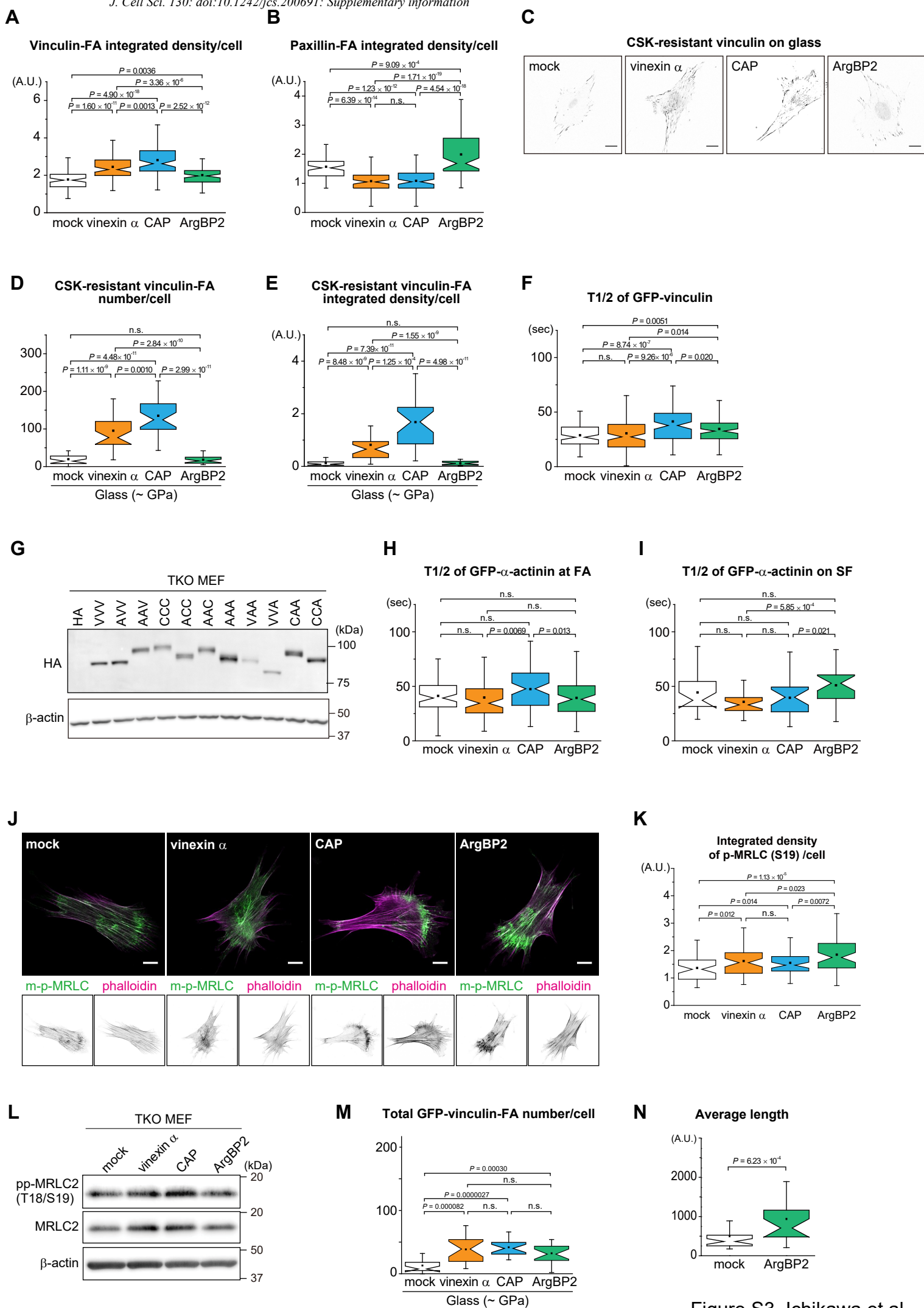
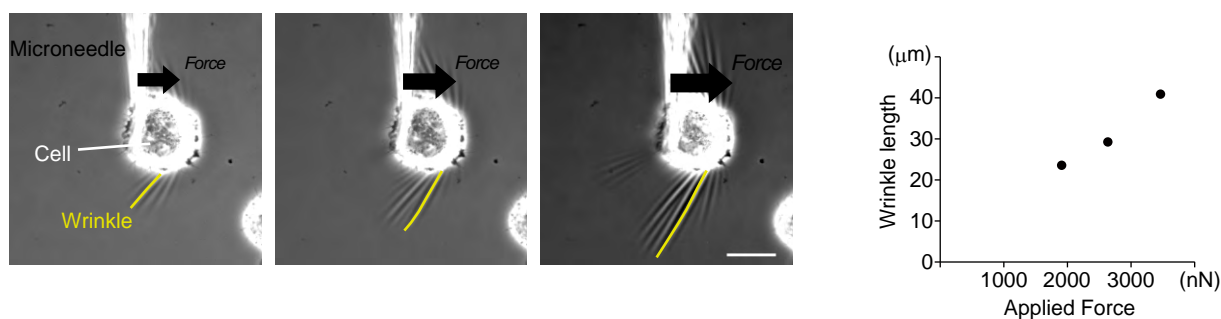


Figure S3, Ichikawa et.al.



**Supplementary figure S3. The effects of SORBS proteins on FA proteins.** (A, B) The integrated density of vinculin-positive FAs (A) and paxillin-positive FAs (B) per cell were quantified from the images in Fig. 3A and B, respectively.  $n=90$ ;  $P$  value calculated by Mann-Whitney U-tests. (C-E) SORBS-reexpressing cells were cultured on coverslips and treated with CSK, followed by immunostaining using anti-vinculin antibody. Thirty individual cells from three separate experiments were photographed for each condition, and the representative images are displayed (C). Scale bars, 20  $\mu\text{m}$ . The number (D) and integrated density (E) of CSK-resistant vinculin-positive FAs per cell were quantified from images ( $n=30$ ).  $P$  value was calculated by Mann-Whitney U-test. (F, H, I)  $T_{1/2}$  was calculated from curve-fitting the data in each FRAP experiment, related to Figs. 5B, 6B and 6E, respectively.  $P$  value was calculated by Mann-Whitney U-tests. (G) Expression of HA-tagged chimeric proteins was examined by immunoblotting using anti-HA antibody. (J, K) SORBS-re-expressing cells cultured on coverslips were immunostained using anti-mono-phosphorylated (S19) antibody with phalloidin staining (J). Scale bars, 20  $\mu\text{m}$ . The integrated density of mono-phosphorylated MRLC per cell was quantified from images of ninety individual cells from three separate experiments (K).  $n=90$ ;  $P$  value calculated by Mann-Whitney U-tests. (L) SORBS-reexpressing cells cultured on collagen coated dishes were lysed and subjected to SDS-PAGE. Total MRLC and di-phosphorylated MRLC (T18/S19) were examined by immunoblotting using the indicated antibodies.  $\beta$ -actin was used as a loading control. (M) SORBS-reexpressing cells stably expressing EGFP-vinculin cultured on coverslips were treated with 3  $\mu\text{M}$  blebbistatin for 135 min, then GFP-fluorescence images were obtained. The number of total GFP-vinculin-positive FAs per cell were quantified from the images.  $n=20$ ;  $P$  value was calculated by Mann-Whitney U-test. (N) Averaged wrinkle length of TKO MEF/mock and TKO MEF/ArgBP2. Cells that did not divide during the 2 hour observation were selected from the experiment of Fig. 8. Total length of wrinkles per cells were quantified at every time points and averaged. The number of cells is  $n=34$  (TKO MEF/mock) and  $n=21$  (TKO MEF/ArgBP2).  $P$  value was calculated by Mann-Whitney U-test.

**A**



**B**

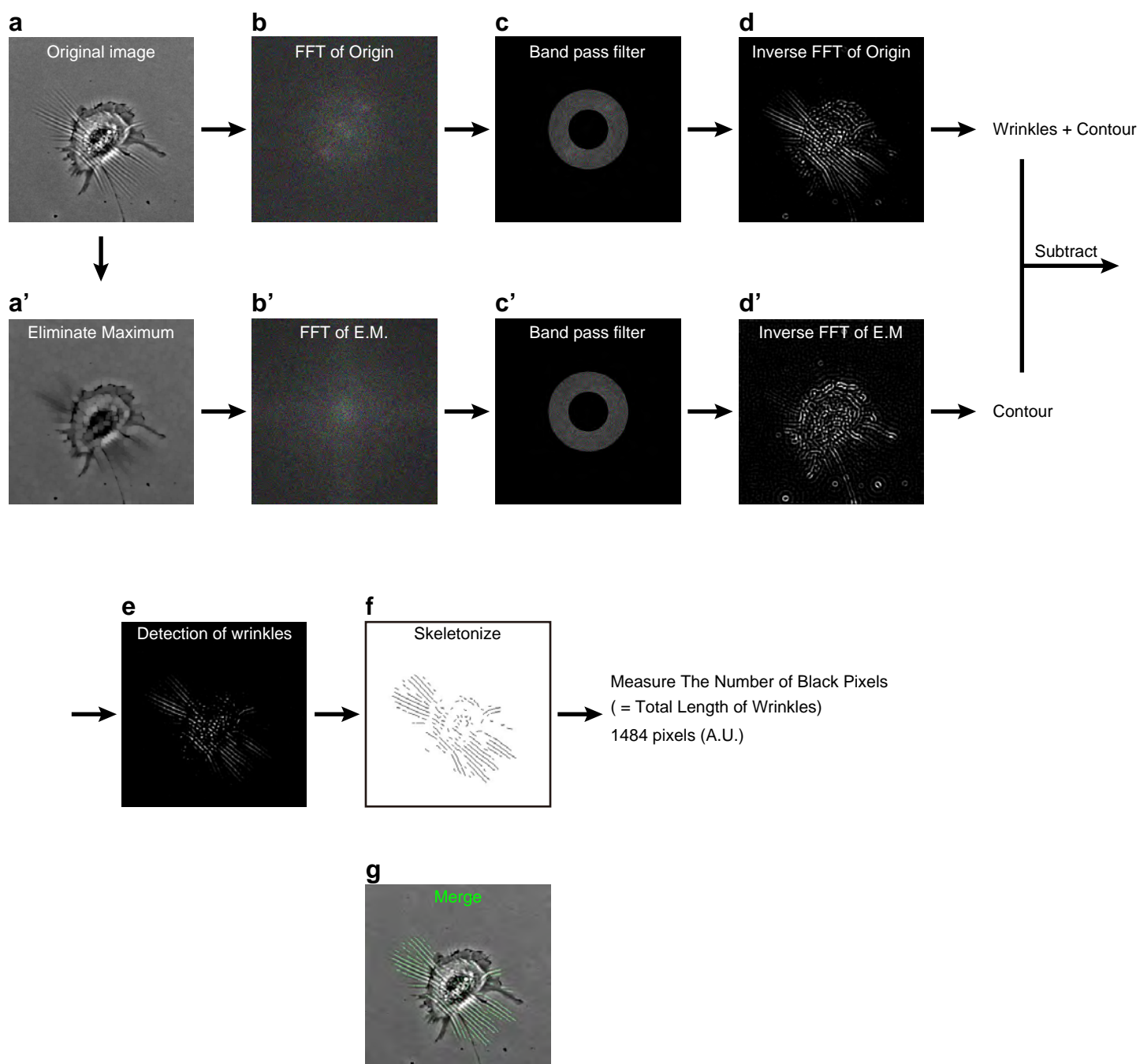
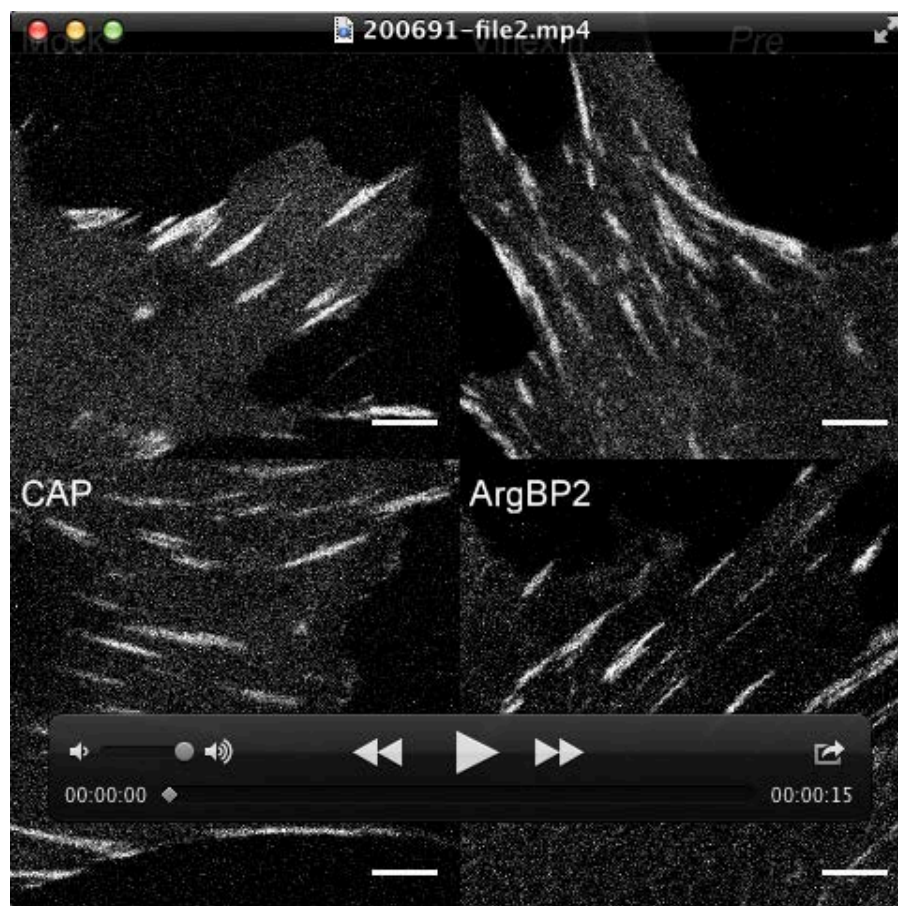


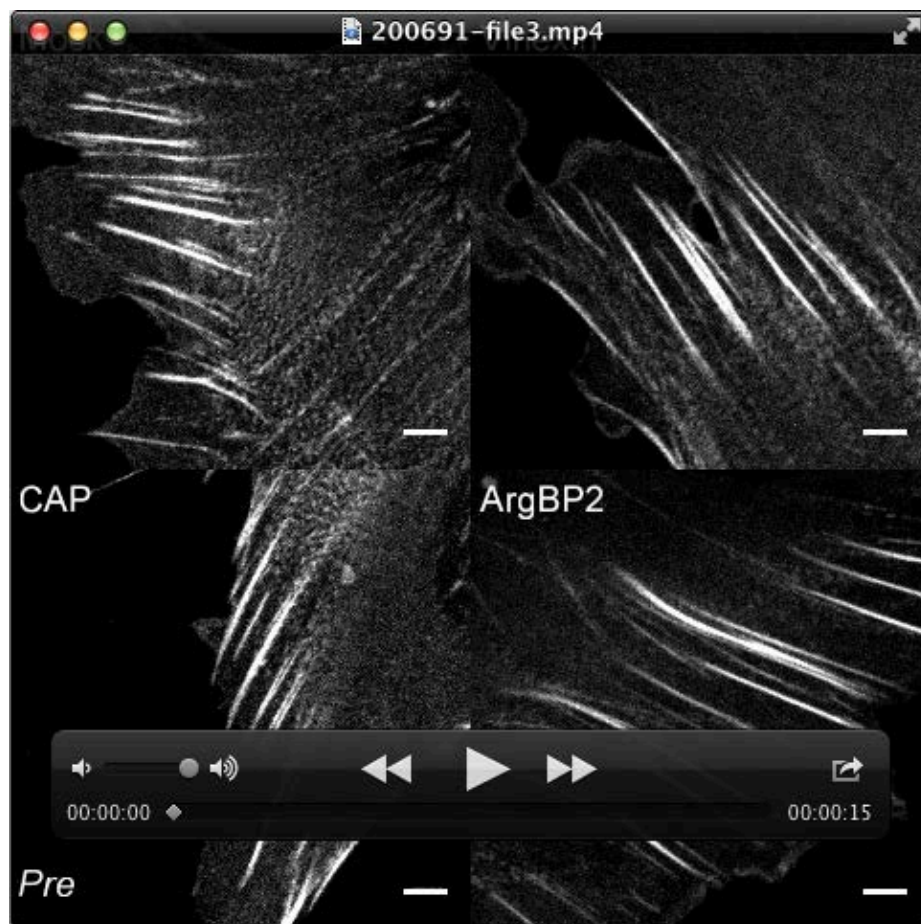
Figure S4, Ichikawa et.al.

**Supplementary figure S4. The automatic detection of wrinkles in cell contraction assay.** (A) We demonstrate using a flexible microneedle that the length of the wrinkles is positively correlated with the forces applied horizontally onto the silicone gel, thus consistent with a previous study (Burton and Taylor, 1997). Here the forces were obtained from the product of the spring constant and deflection of the microneedle. The microneedle, thus used as a force sensor, was made from a glass rod (1 mm in diameter) using a glass-electrode puller (P-97, Sutter Instrument, Novato, USA) to have a tip diameter of  $\sim 5 \mu\text{m}$ . The spring constant was determined to be  $180 \text{ nN}/\mu\text{m}$  based on the cross-calibration method using a commercially available atomic force microscopy cantilever (OMCL-TR400PB-1, Olympus, Tokyo, Japan). For this demonstration, a single glutaraldehyde-fixed MEF was plated on the silicone gel, and forces were applied to the cell within a plane by horizontally moving the base of the microneedle with a micromanipulator (MWO-3, Narishige, Tokyo, Japan). The displacements of the microneedle tip were imaged on a microscope (IX-71, Olympus, Tokyo, Japan) to determine the deflection. Scale bar,  $20 \mu\text{m}$ . (B) Wrinkles generated by the contraction of live MEFs in cell contraction assay were automatically detected by using a custom-made program written in Fiji software. The original image is displayed in (a) and was processed with a command to eliminate high-intensity signals as described in (a'). The images (a, a') were processed with a 2-dimensional fast Fourier transformation (FFT) (b,b'). A band-pass filter was executed to detect the wrinkles, with a spatial period between  $3\text{-}6 \mu\text{m}$  that are typical for the wrinkles generated by MEFs (c,c'). The images (c, c') were then processed with an inverse FFT (d, d'). The resulting images contain both the wrinkles and the contour of cells (d) or only the contour (d'). The image (d') was subtracted from the image (d) to remove the cell contour, and we obtained the image (e) that only contains wrinkles. The total length of the wrinkles was quantified after skeletonization, i.e., line segmentation (f). The merged image of the original image with detected wrinkles indicates that this custom-made program has worked (g).

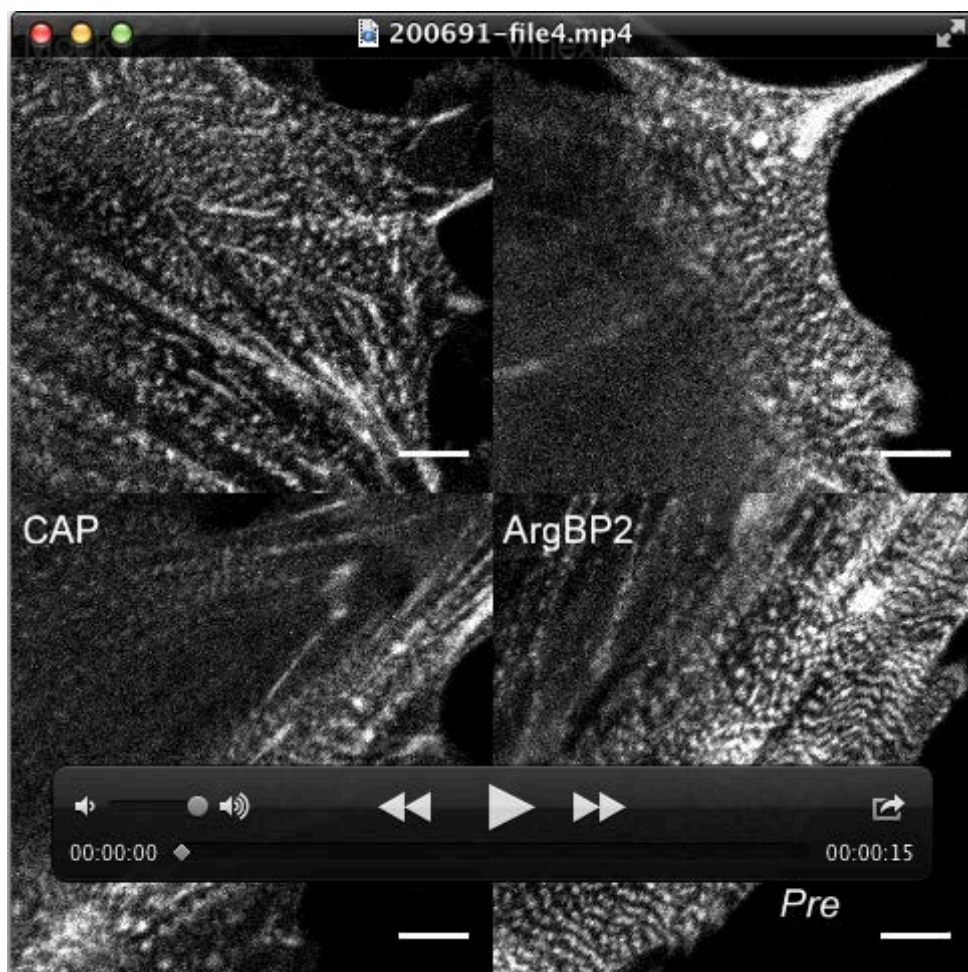




**Movie 1. FRAP analysis of GFP-vinculin at FAs in SORBS-reexpressing cells.** This movie corresponds to Fig. 5A. Images were collected every 5 seconds.



**Movie 2. FRAP analysis of GFP- $\alpha$ -actinin at the proximal end of FAs in SORBS-reexpressing cells.** This movie corresponds to Fig. 7A. Images were collected every 5 seconds.



**Movie 3.** FRAP analysis of GFP- $\alpha$ -actinin on punctate structures along SFs in SORBS-reexpressing cells. This movie corresponds to Fig. 7D. Images were collected every 5 seconds.